

Nonionic Urea Surfactants: Influence of Hydrocarbon Chain Length and Positional Isomerism on the Thermotropic and Lyotropic Phase Behavior

Darrell Wells,[†] Celesta Fong,^{*,†} Irena Krodkiewska,[†] and Calum J. Drummond[‡]

CSIRO Molecular and Health Technologies, Bag 10, Clayton South, Victoria 3169 Australia, and CSIRO Molecular and Health Technologies, P.O. Box 184, North Ryde, New South Wales 1670 Australia

Received: November 14, 2005; In Final Form: January 11, 2006

The thermotropic and lyotropic phase behavior of 1- and 5-decyl urea, and 1-, 2-, 4-, and 6-dodecyl urea have been studied. This allowed the effect of positional isomerism to be examined. Intermolecular hydrogen bonding by the urea moiety is the dominant factor in determining the solid-state thermal behavior and crystal solubility boundary of these linear nonionic surfactants. The positional isomers where the urea moiety was not situated at the terminus of the hydrocarbon chain exhibited higher melting points than the 1-alkyl ureas. This has been rationalized by postulating interdigitated chains in the solid state. In the urea surfactant–water systems, three phases are observed, viz. crystalline solid, a dilute aqueous solution of the alkyl urea, and an isotropic liquid. The last two phases coexist in the low-surfactant, high-temperature region of the binary phase diagram. An overview of structure–property correlations for linear nonionic urea surfactants is presented in light of the new physicochemical data obtained for the decyl urea and dodecyl urea positional isomers.

Introduction

The synthesis of urea in 1828 by Frederick Wohler initiated the age of organic molecular science.¹ After this key historical event, synthetic urea has functioned in many roles. Urea inclusion compounds have served as separation media^{2–5} and have provided an insight into the nature of hydrogen bonding for two-dimensional crystal engineering.^{6–8} The ability of the urea molecule to participate in hydrogen-bonded α -networks via the carbonyl group of one unit and two hydrogen atoms of an adjacent unit (bifurcated hydrogen bonding) provides the supramolecular “cement”. Urea is a chaotropic agent and has progressed the understanding of hydrophobic interaction in aqueous solutions. Urea’s chaotropic behavior has also been utilized to investigate the three-dimensional structure of biopolymers such as proteins.^{9–13} The mechanism behind the chaotropic behavior does, however, remain the topic of some debate. For example, urea is generally referred to as a water structure-breaker, interfering with the hydrogen-bonded network of water,^{14–17} but Wallqvist and co-workers¹⁸ have proposed that urea preferentially adsorbs onto the charged hydrophilic residues of proteins.

Despite widespread interest in urea, there has only been a relatively modest amount of research on the properties of urea-based amphiphiles. While urea itself has very high water solubility (e.g., >20 mol dm^{−3} at 25 °C), nonionic urea surfactants with medium and long hydrocarbon chain substituents have very low water solubility. Insoluble monolayers of urea surfactants, e.g., saturated C12,¹⁹ C16,²⁰ C17,²¹ and C18^{21–25} 1-alkyl urea surfactants, have been used to explore the nature of hydrogen bonding at the air–water interface. These studies have highlighted the reversibly switchable nature of hydrogen bonding in these supramolecular structures. Disruption

of the bifurcated hydrogen bonding has been achieved by substitution of the urea hydrogen with methyl moieties.²⁶ More recently, Seki et al.^{26–28} have observed photomechanical responses in azobenzene–urea surfactant assemblies and have attributed this to the mode of the intermolecular hydrogen bonding. Huo and co-workers²⁹ have also reported Langmuir monolayers of symmetrically disubstituted diacetylene urea molecules. These were of nontraditional architecture with urea-based hydrogen bonding in the center of the molecule resulting in the uncommon situation of the hydrophobic tails being in contact with water.²⁹ Wang et al.³⁰ have recently leveraged this work to produce thermally stable nonlinear optical Langmuir–Blodgett films.

Other aspects of the behavior of this class of nonionic surfactant have received very scant attention in the literature. Wells and Drummond have previously reported some physicochemical properties of the C6, C7, and C8 1-alkyl ureas.³¹ This previous work indicated that strong intermolecular hydrogen bonding in the crystalline state contributed to a relatively low solubility and a high crystal solubility boundary for these urea surfactants. For surfactant–water mixtures in the temperature range 20–98 °C, three phases were observed, viz. a crystalline solid, a dilute aqueous solution of 1-alkyl urea, and an isotropic liquid that was thought to be rich in the 1-alkyl urea while containing water.³² More recent work by this research group has revealed that the dominance of the urea headgroup homointeraction can be ameliorated through judicious modification of the hydrocarbon chain.³² The introduction of either terpenoid or unsaturated hydrocarbon chains encourages the formation of an inverse hexagonal (H_{II}) phase that is thermodynamically stable in excess water.^{32,33}

In the present work, we continue to investigate the influence of the molecular geometry of the hydrocarbon chain on the thermotropic and lyotropic phase behavior of the nonionic urea-based surfactants. In particular, the introduction of positional isomerism is examined in a series of decyl (C10) and dodecyl

* To whom correspondence should be addressed. E-mail: Celesta.Fong@csiro.au. Phone: +61-3-95452608. Fax: 61-3-95452515.

[†] Bag 10, Clayton South.

[‡] P.O. Box 184, North Ryde.

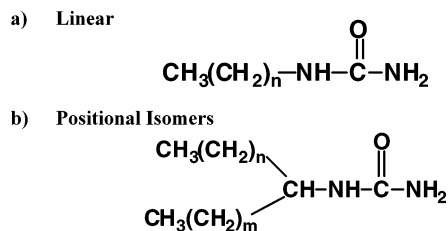


Figure 1. Structural representations of the nonionic urea-based surfactants. (a) 1-Alkyl urea surfactants where $n = 9$ and 11 for 1-decyl and 1-dodecyl, respectively. (b) Positional isomers where $n = 3$ and $m = 4$ for 5-decyl urea; $n = 0$ and $m = 9$ for 2-dodecyl urea; $n = 2$ and $m = 7$ for 4-dodecyl urea; and $n = 4$ and $m = 5$ for 6-dodecyl urea.

(C12) ureas (Figure 1). The thermal properties of the neat materials, solubility in water, and partial binary surfactant–water phase diagrams are reported. The effect of headgroup migration along the hydrocarbon chain is investigated.

Experimental Section

General Syntheses of Alkyl Urea Surfactants. Nitrourea was synthesized by the method of Davis and Blanchard.³⁴ The procedure involves reaction of urea nitrate with concentrated sulfuric acid. The target urea surfactant was formed from reaction of nitrourea and the appropriate amount of amine using the method of Buck and Ferry.³⁵ The detailed synthesis and characterization of the amine precursors and target urea surfactants are provided as Supporting Information.

Infrared (IR) Spectroscopy. IR spectroscopy was performed using a BOMEM MB 101 from Extech Equipment Pty. Ltd. Spectra were recorded at room temperature in the range $4000\text{--}500\text{ cm}^{-1}$ and were accumulated for four scans at a resolution of 4 cm^{-1} . The material was examined as either pellets of compressed potassium bromide or as a loose powder mixed with potassium bromide using the Harrick diffuse-reflectance accessory. Samples were also examined in chloroform and carbon tetrachloride solution using a 0.1 mm thick sodium chloride cell, for which the background was compensated.

Differential Scanning Calorimetry (DSC). DSC was performed using a Mettler 3000 system at scan rates of either 2.5 or $0.1\text{ }^{\circ}\text{C/min}$. The temperature calibration ($\pm 0.3^{\circ}\text{C}$) of the platinum thermometer was performed with ultrahigh purity 1-hexane, water, and indium. The thermal calibration of the DSC instrument was performed by integration of the standard indium melting endotherm. The energies of the transitions were calculated by the Mettler 3000 software.

Binary Phase Behavior at Low Urea-Based Surfactant Concentrations. Surfactant urea–water mixtures were prepared by weighing an amount of solid into 12 mm screw cap tubes and adding water by weight. The urea surfactant was first dissolved (as much as possible) by heating the samples near $100\text{ }^{\circ}\text{C}$ prior to precipitation by cooling. The heating rate was $<2\text{ }^{\circ}\text{C/min}$ in a water bath with continuous stirring. The temperature was measured against a certified thermometer immersed in the center of the sample. The sample mixtures were viewed against a matte black background through a magnifying lens ($1.5\times$ magnification) with side illumination. Each sample was cooled and heated through several cycles to accurately determine the transition point. The actual phases of the transitions were determined from the water penetration experiments. The transition temperatures refer to the heating runs.

Water Penetration into Urea-Based Surfactants. Solid urea was melted between a microscope slide and cover slip and allowed to cool to room temperature prior to addition of water at the edge of the cover slip. Capillary action drew the water

between the two glass surfaces, surrounding the solid material. The sample was heated at $2\text{ }^{\circ}\text{C/min}$ in the Mettler FP82HT hot stage controlled by a FP90 central processor. The interaction of water with the solid urea-based surfactant was viewed using an Olympus IMT-2 microscope equipped with crossed polarizing lenses.

Results and Discussion

IR Analyses. IR spectra were obtained for each of the urea-based surfactants in several different media. They were compressed crystalline material in a KBr disk, diffuse reflectance of crystalline material as a loose powder with KBr, and solutions with chloroform and carbon tetrachloride. The solubility of the urea surfactants in carbon tetrachloride is poor, and these were examined as saturated solutions.

The extent of hydrogen bonding in the urea-based surfactants has been qualitatively assessed using IR spectroscopy. A shift in frequency of an associated band (solid state) from that of a band in solution with reduced crystal–crystal interactions (e.g., carbon tetrachloride) provides evidence for the existence of intermolecular hydrogen bonding and an indication of the strength of this interaction. Typically, hydrogen bonding moves the stretching bands to lower frequencies (wavenumbers), often with increased intensity and broadening of the peak.³⁶ For this purpose, the N–H region between $\sim 3100\text{--}3500\text{ cm}^{-1}$ (ν_{NH}) and the amide region between 1500 and 1700 cm^{-1} are the most instructive (Figure 2a). The amide region incorporates three distinct peaks corresponding to stretching vibrations of the amide I (C=O) at $\sim 1650\text{ cm}^{-1}$ and the amide II (C–N) at $\sim 1530\text{ cm}^{-1}$, as well as a bending mode $\delta(\text{N–H})$ at $\sim 1600\text{ cm}^{-1}$.^{37–40}

The ν_{NH} absorptions are convoluted. For a series of monoalkyl ureas in chloroform, Mido and co-workers distinguish three N–H stretching vibrations, with an asymmetric component at $\sim 3515\text{ cm}^{-1}$ ($\nu_{\text{as}}(\text{NH}_2)$), a symmetric stretch at $\sim 3415\text{ cm}^{-1}$ ($\nu_{\text{s}}(\text{NH}_2)$), and $\nu(\text{N–H})$ at intermediate frequencies between these.³⁹ This latter stretching peak is attributed to the N–H moiety adjacent to the alkyl substituent. The amide I occurs at lower frequencies than carbonyl groups in ketones and aldehydes due to the resonance stabilization of the urea, leading to a lengthening of the C=O bond.³⁷ Mido et al. have shown that, for urea and several mono- and dialkyl derivatives, the amide II band is not a pure vibration but is also coupled to the N–H deformation, $\delta(\text{NH})$.^{38–40} Table 1 lists the N–H (ν_{NH}), C=O (amide I), and C–N (amide II) stretching frequencies and δ -(N–H) deformation mode in the solid state, in chloroform, and in carbon tetrachloride. While solvent effects are not an issue for carbon tetrachloride solutions, in chloroform, hydrogen bonding exists between the C=O of the urea moiety and the protons of the solvent.

In previous studies³¹ of short-chain C6, C7, and C8 1-alkyl ureas, a progressive shift toward higher spectral frequencies for each of the ν_{NH} and amide I stretching vibrations from the solid to dissolution in chloroform was observed. This was attributed to a weakening of the intermolecular hydrogen bonding between urea headgroups. The ν_{NH} band of the 1-alkyl ureas is convoluted in the solid state with a main peak at $\sim 3390\text{ cm}^{-1}$ and a broad shoulder on the low-frequency side. A weak peak at $\sim 3210\text{ cm}^{-1}$ is also observed. The amide I and amide II bands occur at ~ 1660 and $\sim 1530\text{ cm}^{-1}$, respectively, in the solid state. Interestingly, the amide II band does not shift with polarity of the solvent, while the amide I band experiences a large shift toward higher wavenumbers ($\sim 1700\text{ cm}^{-1}$) with solvent environment.

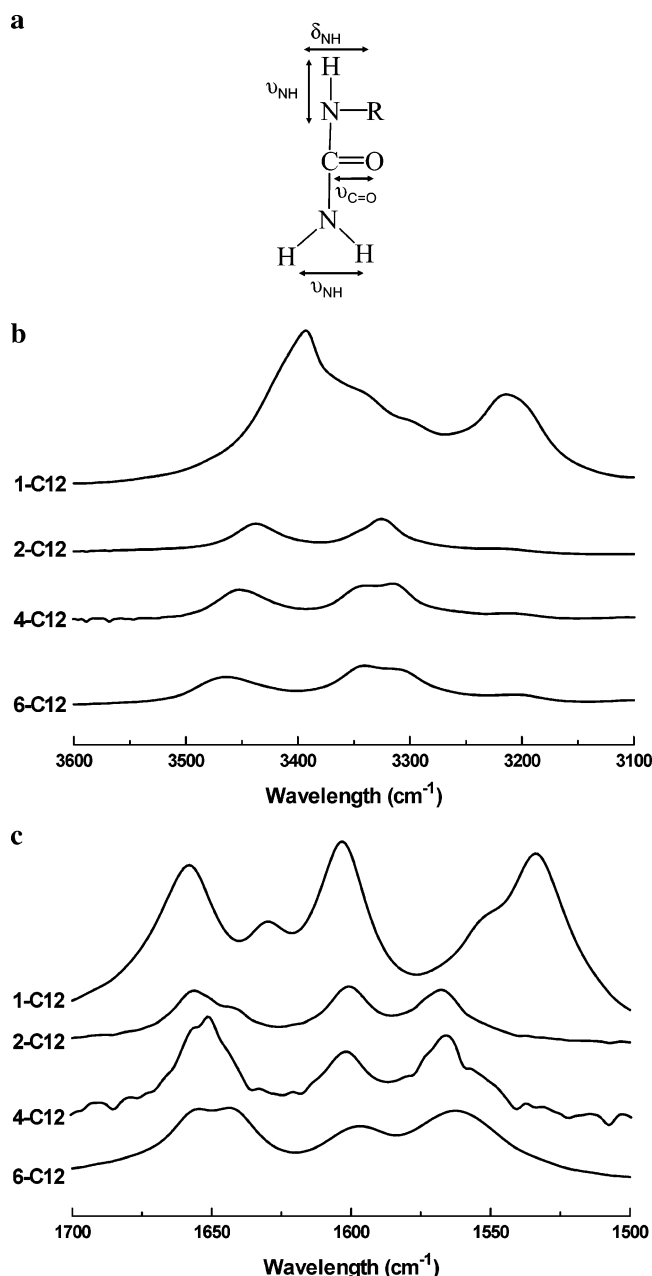


Figure 2. IR spectra. (a) Direction of transition moments of each of the IR signals from the urea surfactants, (b) the N–H region of the dodecyl urea family as solid material in KBr disk, and (c) the amide region of the dodecyl urea family of ureas as solid material in KBr disk.

For the crystalline 1-decyl and 1-dodecyl ureas of the current study, qualitatively similar vibrational frequencies were observed in the IR spectra in KBr matrix. However, a comparison of the pertinent regions reveals distinct differences between the 1-alkyl homologues and the other positional isomers. In particular, for the dodecyl urea isomers, the IR spectrum resolves two broad peaks in the N–H region (Figure 2b,c). ν_{NH} increases from 3394 to 3464 cm^{-1} with the magnitude of $\Delta\nu$ increasing with the symmetry of the hydrophobe from 1- to 2- to 4- to 6-dodecyl urea. A shoulder at $\sim 3330 \text{ cm}^{-1}$ in the parent 1-alkyl urea is better resolved in the isomers, while the peak at $\sim 3210 \text{ cm}^{-1}$ is much reduced in intensity. The amide I and $\delta(\text{N–H})$ bands remain relatively unchanged, though there is a large shift in the amide II peak toward higher wavenumbers ($\sim 30 \text{ cm}^{-1}$) from 1- to 2- to 4- to 6-dodecyl urea. The magnitude of the shift is not dependent upon the position of the headgroup along the

TABLE 1: Characteristic IR Frequencies for the Alkyl Ureas (in cm^{-1})

surfactant	environment	ν_{NH}	amide I	amide II
1-decyl urea	solid KBr	3393, 3210	1657	1533
	solid powder	3388, 3208	1654	1535
	chloroform ^d	3520, 3415	1675	1532
	chloroform ^b	3515, 3410	1675	1531
	carbon tetrachloride ^c	3513, 3442, 3414	1702	—
5-decyl urea	solid KBr	3445, 3332, 3207	1652	1561
	solid powder	3433, 3324	1649	1558
	chloroform ^d	3510, 3426	1672	1521
	chloroform ^e	3510, 3423	1672	1523
	carbon tetrachloride ^f	3512, 3436, 3413, 3327	1699	—
1-dodecyl urea	solid KBr	3394, 3211	1657	1534
	solid powder	3380, 3210	1653	1536
	chloroform ^g	3515, 3420	1676	1532
	chloroform ^h	3517, 3418	1675	1531
	carbon tetrachloride ⁱ	3514, 3434, 3415	1698	—
2-dodecyl urea	solid KBr	3432, 3326, 3218	1656	1523
	chloroform ^j	3520, 3426	1674	1569
4-dodecyl urea	solid KBr	3450, 3336, 3312	1647	1562
	chloroform ^k	3519, 3425	1664	1557
	carbon tetrachloride ^l	3520, 3431, 3409	1698	—
6-dodecyl urea	solid KBr	3464, 3331, 3201	1649	1562
	solid powder	3459, 3331	1646	1559
	chloroform ^m	3520, 3415	1673	1525
	chloroform ⁿ	3515, 3421	1672	1526
	carbon tetrachloride ^o	3515, 3441, 3418	1700	—

^a $4.5 \times 10^{-3} \text{ mol dm}^{-3}$. ^b $2.3 \times 10^{-2} \text{ mol dm}^{-3}$. ^c $< 3.8 \times 10^{-3} \text{ mol dm}^{-3}$, saturated solution. ^d $6.9 \times 10^{-3} \text{ mol dm}^{-3}$. ^e $< 3.5 \times 10^{-2} \text{ mol dm}^{-3}$, saturated solution. ^f $< 7.3 \times 10^{-3} \text{ mol dm}^{-3}$, saturated solution. ^g $4.9 \times 10^{-3} \text{ mol dm}^{-3}$. ^h $< 2.2 \times 10^{-2} \text{ mol dm}^{-3}$, saturated solution. ⁱ $< 4.4 \times 10^{-3} \text{ mol dm}^{-3}$, saturated solution. ^j $1.9 \times 10^{-3} \text{ mol dm}^{-3}$. ^k $< 2.2 \times 10^{-2} \text{ mol dm}^{-3}$, saturated solution. ^l $< 4.4 \times 10^{-3} \text{ mol dm}^{-3}$. ^m $4.4 \times 10^{-3} \text{ mol dm}^{-3}$. ⁿ $2.2 \times 10^{-2} \text{ mol dm}^{-3}$. ^o $< 6.5 \times 10^{-3} \text{ mol dm}^{-3}$, saturated solution.

chain. An increase in ν_{NH} reflects the steric bulk of the growing double chain as the urea headgroup is advanced toward the center^{37–40} and suggests a weakening of the intermolecular hydrogen bonding between urea headgroups in the isomers.

In solution, bands at ~ 3515 and 3415 cm^{-1} are resolved that are due to asymmetric ($\nu_{\text{as}}(\text{NH})$) and symmetric ($\nu_{\text{s}}(\text{NH})$) stretches with an additional band at intermediate frequencies of $\sim 3440 \text{ cm}^{-1}$ in carbon tetrachloride due to $\nu(\text{NH})$ as described above. Variation of the surfactant concentration in chloroform produces little change in the observed vibrational spectra. The effect of changing solvent environment produces a shift to higher wavenumbers of the ν_{NH} and amide I while the $\delta(\text{N–H})$ remains invariant. Interestingly, the amide II vibrations show different effects which are dependent upon the position of the headgroup. In the linear surfactants where the headgroup is at the terminus of the chain, the amide II band is invariant with solvent. However, for the positional isomers, a large shift of the amide II band is observed toward lower wavenumbers ($\sim 40 \text{ cm}^{-1}$). This is interpreted as the low contribution of the resonance structure to hydrogen bonding in the positional isomers.

Recently, Hashimoto and co-workers⁴¹ have determined the crystal structures of several medium-chain-length 1-alkyl ureas including 1-decyl and 1-dodecyl urea. X-ray crystallography at near-ambient temperatures confirms the presence of a hydrogen-

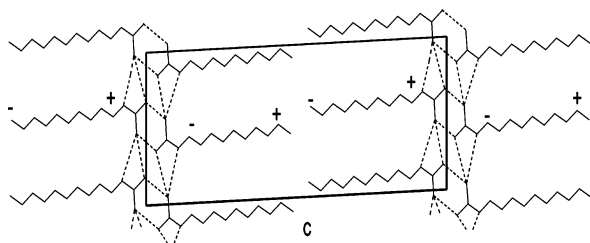


Figure 3. X-ray crystal structure of 1-decyl urea at 296 K showing head-to-tail arrangement (lamellar) of the supramolecular structures along a projection of the *ac* plane (reproduced with permission from Hashimoto et al.).⁴¹ The '+' indicates the alkyl chain points out of the *ac* plane, while the '-' sign indicates the alkyl group points into the plane of projection.

bond network which results in two-dimensional, platelike supramolecular structures with a crossed arrangement of alkyl groups caused by a twist of the urea chain.⁴¹ The unit cell incorporated the stacking of these supramolecular structures along the *a* axis to form lamellae-type surfaces (Figure 3). Similar chain conformations have been identified in aliphatic amides.⁴²

Energy-minimized structures of the family of dodecyl urea isomers suggest an increasing V-shaped conformation of the hydrophobe as the urea moiety migrates toward the center of the molecule (Figure 4). On the basis of these constructs of single molecules in vacuo, it is anticipated that the lamellar stacking of the 1-alkyl ureas, identified by Hashimoto et al.,⁴¹ would be severely disrupted. Indeed, the IR spectra of the positional isomers, where the urea headgroup is located away from the end of the chain, in the solid-state, suggests a weakening of the urea moiety intermolecular hydrogen bonding as compared to the 1-alkyl analogue. Interestingly, however, the melting points of these isomers are higher than that of the 1-alkyl ureas (vide infra).

DSC. DSC scans for each of the urea-based surfactants are presented in Figure 5. Table 2 lists the melting point transition temperatures and enthalpies for the transitions, together with melting points obtained from visual observations using optical microscopy. The transition temperature has been taken from the peak maxima of the endotherm. Data for the C6, C7, and C8 1-alkyl ureas reported previously³¹ have been included in Table 2 for comparison.

The melting point is not appreciably affected by increasing the hydrocarbon chain length from C6 to C12 in the 1-alkyl urea surfactants. Indeed, several workers have reported relatively invariant melting points for a series of 1-alkyl ureas ranging from C4 to C22.^{31,41,43} This suggests that it is the urea homo-interaction that dominates the melting behavior with only a minor contribution from the alkyl chain. Further, for a homologous series of linear C6–C18 compounds, the melting point sequence is 1-alkane < 1-alkanol < 1-alkylamine < 1-alkanoic acid < 1-alkanamide \approx 1-alkyl urea.⁴⁴ Therefore, the substituted urea interaction is similar to the substituted amide, suggesting that it is the amide component of the urea moiety that dominates the melting behavior. Nevertheless, the enthalpy associated with this transition is significantly greater for 1-decyl urea and 1-dodecyl urea compared to the shorter-chain relatives.

Typically, for a homologous series of aliphatic compounds, deviation from the straight-chain structure has the effect of lowering the melting point.^{45,46} For other nonionic surfactants, such as the positional isomers dodecyl β -D-glucosides, this leads to a lowering of the solid-state melting point and the Krafft temperature in water.⁴⁷ However, for the alkyl ureas, the opposite trend is observed, namely that positional isomerism in the short chain C3 and C4 ureas results in an increase in the melting point behavior.⁴³ This phenomenon is also observed with the C10 urea isomers with the melting point of 5-decyl urea increased by 28 °C over 1-decyl urea. For the family of

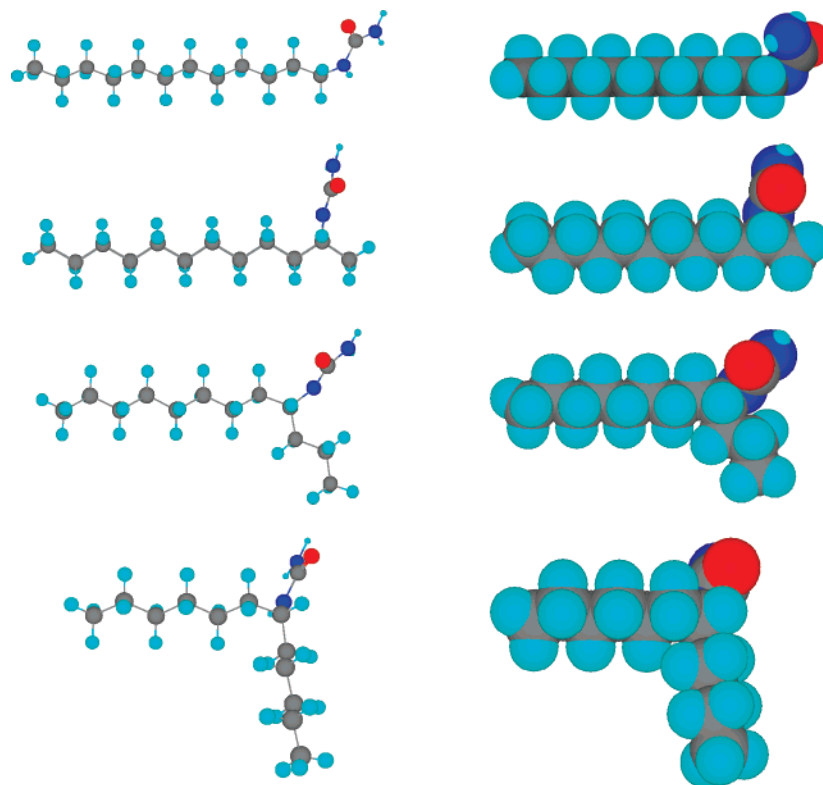


Figure 4. Ball-and-stick and space-filling structural representations of (from top to bottom) 1-dodecyl urea, 2-dodecyl urea, 4-dodecyl urea, and 6-dodecyl urea.

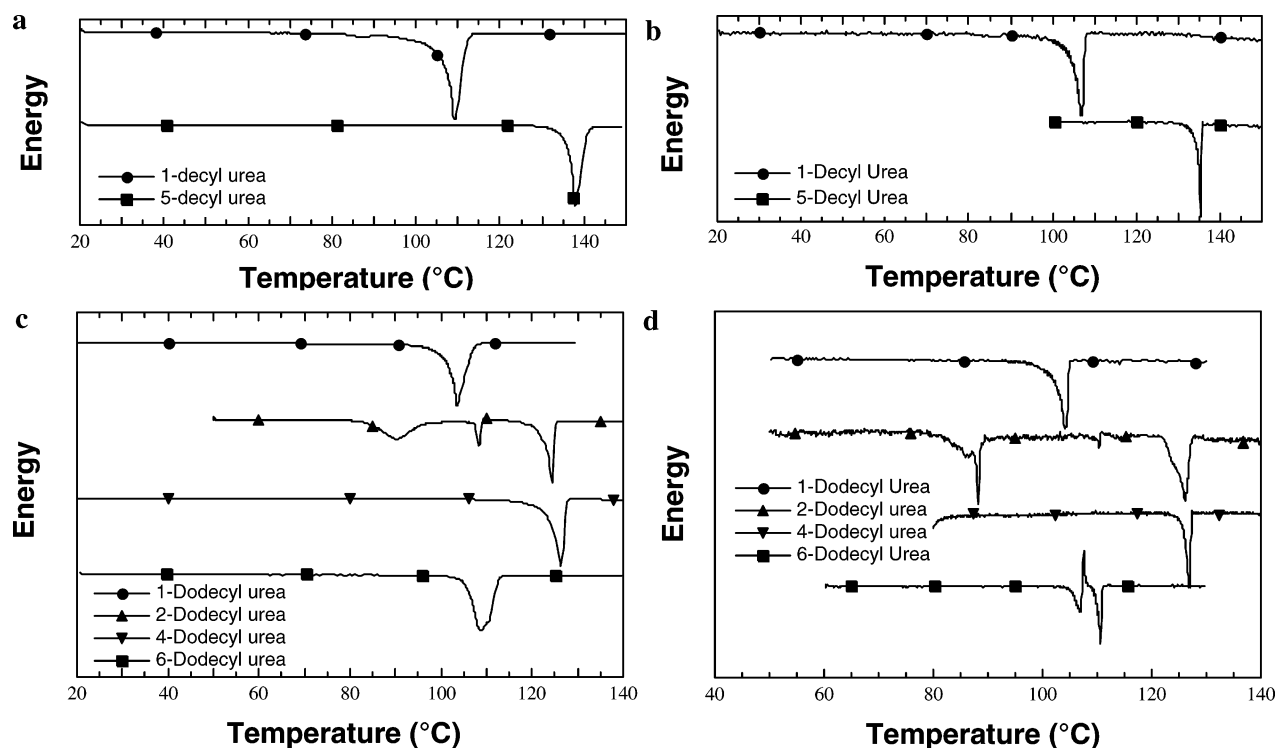


Figure 5. DSC plots showing (a) decyl ureas measured at 2.5 °C/min; (b) decyl ureas measured at 0.1 °C/min; (c) dodecyl ureas measured at 2.5 °C/min; and (d) dodecyl ureas measured at 0.1 °C/min.

TABLE 2: Some Physicochemical Properties of the Alkyl Ureas

surfactant	DSC transition temperature (°C)	DSC temperature (°C)	DSC transition enthalpy (kJ mol ⁻¹)	visual m.p. (°C) ^f	solubility (mol dm ⁻³)		ΔG_s° (kJ mol ⁻¹)		CST points (°C)	
					25 °C	65 °C	25 °C	65 °C	0.01%	0.1%
1-hexyl urea	110 ^a , 107 ^b	108 ^a	-21.5 ^a -26.5 ^b	109-110	7.6×10^{-3}	6.8×10^{-2}	-22.1	-18.9	< 23	23
1-heptyl urea	110 ^a , 109 ^b (106) ^{b,c}	107.8 ^a	-29.4 ^a , -26.3 ^b (-1.4) ^{b,c}	112-113	3.8×10^{-4}	7.6×10^{-3}	-29.5	-25.0	< 23	43
1-octyl urea	99 ^a (79) ^{a,c} , 99 ^b (77) ^{b,c}	96 ^a , 76 ^{a,c}	-23.9 ^a (-11.7) ^{a,c} , -24.6 ^b (-11.4) ^{b,c}	100-102	— ^e	5.5×10^{-3}	— ^e	-26.0	35	66
1-decyl urea	109 ^a (88) ^{a,c} , 107 ^b	106 ^a (84) ^{a,c}	-36.9 ^a (-1.0) ^{a,c} , -32.8 ^b	110-112	— ^e	2.4×10^{-4}	— ^e	-34.8	80	87 ^d
5-decyl urea	138 ^a	136 ^a	-22.6	138-140	— ^e	— ^e	— ^e	—	>100 ^d	>100 ^d
1-dodecyl urea	103 ^a , 104 ^b	91 ^a	-45.7 ^a , -44.7 ^b	103-105	— ^e	5.4×10^{-5}	— ^e	-39.0	89 ^d	89 ^d
2-dodecyl urea	126.8 ^a (93) ^{a,c} (110.7) ^{a,c}	124 ^a (87) ^{a,c} (110) ^{a,c}	-25.4 ^a (-22.6) ^{a,c} (-7.3) ^{a,c}	121-127	— ^e	1.8×10^{-4}	— ^e	-35.4	95 ^d	95 ^d
4-dodecyl urea	126.4 ^e	124 ^a	-30.4 ^e	126-128	— ^e	8.0×10^{-6}	— ^e	~40.9	>100	>100
6-dodecyl urea	110 ^a , 111 ^b (107) ^{b,c}	106 ^a	-25.3 ^a , -16.2 ^b (-12.3) ^{b,c}	112-114	— ^e	1.0×10^{-4}	— ^e	-32.9	87	94 ^d

^a Determined from DSC scanned at 2.5 °C/min. ^b Determined from DSC scanned at 0.1 °C/min. ^c Values in parentheses refer to a transition that occurs before the crystal-isotropic liquid transition. ^d Transition temperature referring to change from crystalline solid to isotropic alkyl urea rich liquid. ^e Smallest amount of material able to be observe with our technique showed no solubility, so solubility was less than 5×10^{-5} mol dm⁻³ from visual observation. ^f Melting point as determined visually from light microscopy.

dodecyl urea isomers, similar trends were observed. Specifically, 2- and 4-dodecyl urea have similar melting points which are about 22 °C higher than 1-dodecyl urea, while 6-dodecyl urea has a melting point about 7 °C higher. The enthalpy of the transition for the positional isomers is of the same order of magnitude as that of the C6, C7, and C8 1-alkyl ureas. Intermolecular hydrogen bonding between headgroups has been identified as a dominant factor in the thermal behavior of neat urea-based surfactants. Dispersion forces, however, also clearly play a role.

We tentatively rationalize the melting point behavior of the positional isomers in terms of the interdigitation of the hydrocarbon chains. However, at this stage, without X-ray crystallographic data for these particular urea-based surfactants, we can only speculate.

In addition to the melting point transition, several other features are present in the DSC traces. The 1-decyl urea has a broad endotherm with a shoulder on the low-temperature side of the main crystal-isotropic liquid transition. This commenced

at 82 °C (0.98 kJ/mol; peak at 87.5 °C) and overlapped with the main endotherm. A similar phenomenon was observed for the 1-hexyl and 1-heptyl ureas reported elsewhere.³¹ In the slow scans, the 'pre-transition' observed for the 1-decyl urea has disappeared due to a smearing of the peak intensity over the small step size. The 6-dodecyl urea appeared as a double maximum, which was resolved at high resolution with scans performed at 0.1 °C/min (Table 2). 2-Dodecyl urea displayed several pre-transitions with maxima at 93, 111, and 127 °C (22.6, 7.3, and 25.4 kJ/mol, respectively). The remainder of the ureas exhibited only a dominant broad endotherm with no pre-transition.

Linear alkanes and long-chain alcohols are known to exhibit rotator or plasticlike phases associated with high-temperature order-disorder transitions occurring at temperatures just below the melting point. For the linear alkanes, these transitions are characterized by transition entropies ($\Delta_{\text{trs}}S$) that are on the order of about one-third to one-half of the entropy of melting ($\Delta_{\text{fus}}S$).⁴¹ Recently, Hashimoto and co-workers⁴¹ have reported quasi-

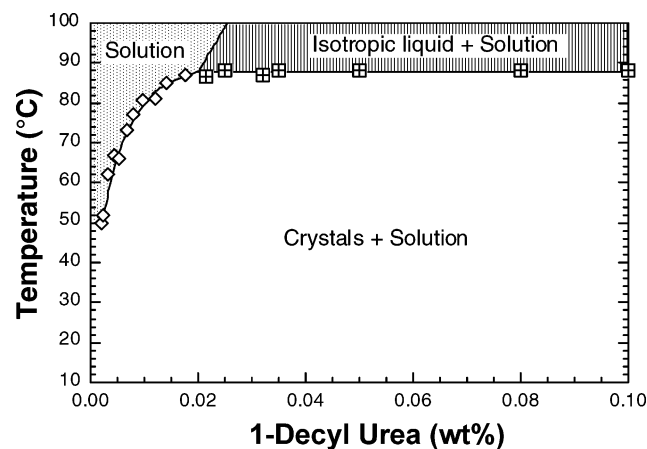


Figure 6. Partial phase diagram for the 1-decyl urea–water system.

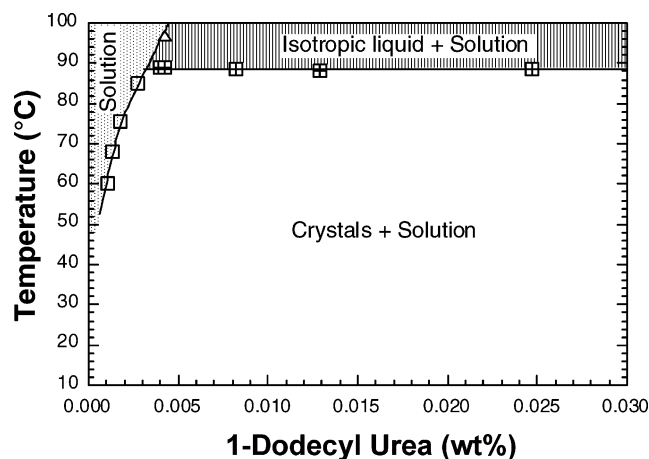


Figure 7. Partial phase diagram for the 1-dodecyl urea–water system.

plastic phases for butyl and octyl ureas and Wells and Drummond³¹ have also previously noted such a pre-transition in octyl urea. The pre-transition occurring at 111 °C in 2-dodecyl urea is postulated to be similar to such phases since $\Delta_{\text{trs}}S/\Delta_{\text{fus}}S = 0.3$. In the current study, no further attempt is made to identify the other features in the DSC traces. However, X-ray crystallographic studies of several alkyl ureas by Hashimoto et. al. have attributed such phase transitions to shifts within the supramolecular framework.

Binary Phase Behavior at Low Urea-Based Surfactant Concentration. Partial urea surfactant–water phase diagrams at low surfactant concentrations are shown in Figures 6–10. The standard free energy of solution ($\Delta G^\circ_{\text{sol}}$) is given by

$$\Delta G^\circ_{\text{sol}} = -RT \ln S \quad (1)$$

where $\Delta G^\circ_{\text{sol}}$ is the free energy involved in the transfer of 1 mol of urea surfactant from dilute aqueous solution to the crystalline state, R is the gas constant, T is the absolute temperature, and S is the mole fraction of the surfactant at the solubility limit. Table 2 lists the solubilities and the $\Delta G^\circ_{\text{sol}}$ values calculated for each of the urea-based surfactants at 25 and 65 °C where appropriate.

There is a steady decrease in the solubility of the n -alkyl ureas as the chain length is increased. For the urea compounds with alkyl chain length C6, C8, C10, and C12, the standard free energy of solution at 65 °C is, to a good approximation, linearly related to the number of carbon atoms n such that:

$$\Delta G^\circ_{\text{sol}} = 1.42 - 3.46n \text{ kJ/mol} \quad (2)$$

with a linear correlation coefficient of 0.992.

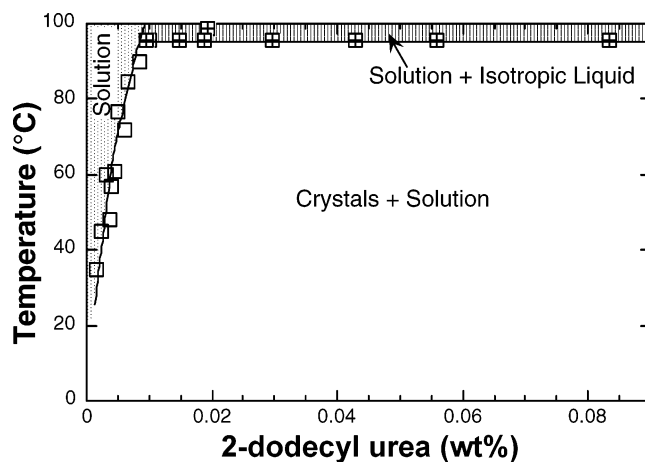


Figure 8. Partial phase diagram for the 2-dodecyl urea–water system.

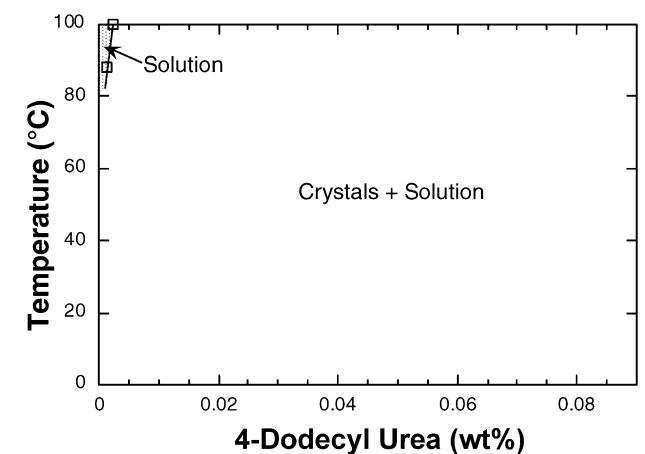


Figure 9. Partial phase diagram for the 4-dodecyl urea–water system.

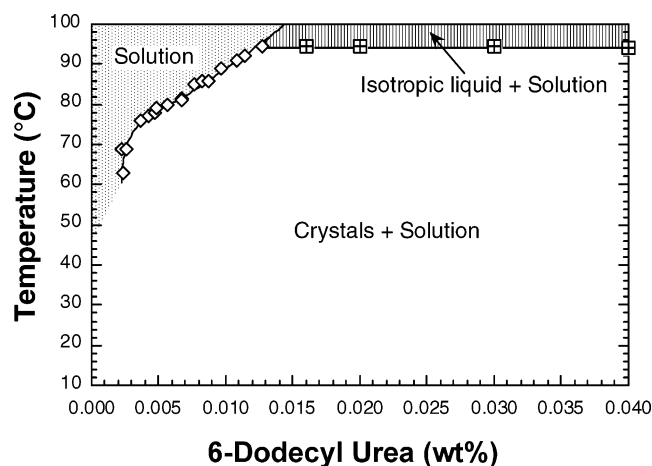


Figure 10. Partial phase diagram for the 6-dodecyl urea–water system.

Hence, the free energy increment for transferring a methylene group, $\Delta G^\circ_{(\text{CH}_2)}$, in a 1-alkyl urea from dilute aqueous solution to the solid state can be taken to be about 3.5 kJ/mol. Table 3 compares the increment associated with analogous events for several types of nonionic molecules from dilute aqueous solution to a different state, as listed in the literature. The differences can be ascribed to the transferral to states with different degrees of hydrocarbon chain order and configurational entropy. For instance, the difference in $\Delta G^\circ_{(\text{CH}_2)}$ for the transfer from water to a hydrocarbon solvent for the 1-alkanes and the air–water interface or to the micellar state may be attributed (in part) to a loss in entropy resulting from orientation of the amphiphiles

TABLE 3: Standard Free Energy Associated with the Transfer of a Methylene Group from Dilute Aqueous Solution

transfer of methylene group to	$\Delta G^\circ_{(\text{CH}_2)}$ kJ/mol
crystalline state for 1-alkyl urea	-3.5
organic liquid for	
1-alkanes	-3.7 ^a
1-alkanoic acids/ 1-alkanols	-3.4 ^{a,b}
monolayer at the air/water interface	-3.3 ^b
micellar state for alkyl ethoxylates	-2.8 ^c

^a Reference 45. ^b Reference 48. ^c Reference 49.

at the interface. Interestingly, the value of $\Delta G^\circ_{(\text{CH}_2)}$ for the 1-alkyl ureas is similar to that observed for a monolayer at the air–water interface and to water/alkanol transfer processes.

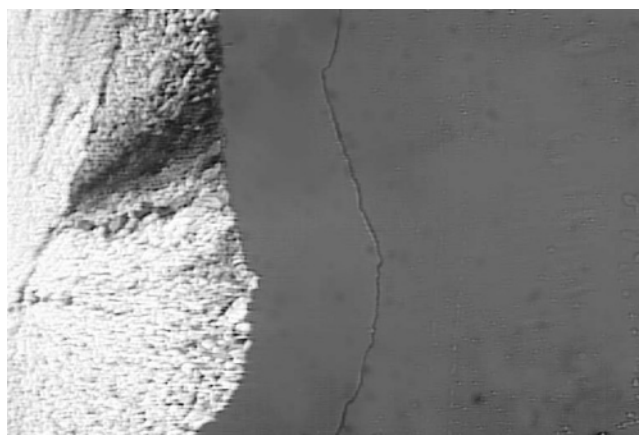
The urea surfactants examined in the current (Figures 6–10) and previous work³¹ exhibit a crystal solubility boundary. The 0.01 and 0.1 wt% crystal solubility transition (CST) points are listed in Table 2. In general, the solubility of the urea-based surfactants is very low, even at elevated temperatures. The alkyl urea–water phase behavior in the low-surfactant region resembles that of the C6–C8 analogues reported elsewhere,³¹ viz. at low temperatures and low surfactant concentration, a mixture of crystals in solution coexists, becoming a true solution at relatively high temperature. In the higher-surfactant-concentration region and at high temperatures, two isotropic liquids phases coexist.

Although the melting points for the C6–C12 1-alkyl ureas are relatively invariant, solubility decreases with alkyl chain length to the extent that, for the 1-alkyl ureas of greater length than C7, no solubility is measured at 25 °C. 2- and 6-dodecyl urea manifest slightly higher solubility at 65 °C than 1-dodecyl urea, while the solubility of 4-dodecyl urea is significantly less than 1-dodecyl urea.

Lyotropic Phase Behavior. Water-penetration studies at the interface of the solid material and water provide information on the phase behavior of concentrated surfactant systems. As water penetrates the solid surfactant, a concentration gradient is established and, provided that the crystal solubility (CST) or Krafft temperature is attained, liquid–crystalline phases may be observed.

In general terms, the water-penetration behavior of the surfactant–water mixtures of the C10 and C12 ureas closely resemble the behavior of their C6–C8 relatives.³¹ Three phases have been identified, viz., a crystalline solid, a dilute aqueous solution of alkyl urea, and a mobile isotropic liquid. The aqueous solution and isotropic liquid coexist in the low-surfactant, high-temperature region of the phase diagram, consistent with observations of the behavior at dilute surfactant concentrations described above. The mobility of the isotropic liquid indicated that this phase is not cubic, but either a reverse micellar phase or a true solution of water in the urea. No attempt was made to further characterize this phase. Anisotropic phases were not observed for any of these surfactants, suggesting higher-order liquid–crystalline phases are not formed under the conditions investigated.

Specifically, for 1-decyl urea, insignificant dissolution of the interface occurred until 87 °C, at which point a mobile isotropic phase developed (Figure 11). No further phases were observed for temperatures up to 98 °C. Crystal solubility temperatures for 1-, 2-, and 6- dodecyl urea were slightly higher at 89, 95, and 97 °C, respectively. However, for 5-decyl and 4-dodecyl urea, an isotropic liquid phase was not observed below the boiling point of water. Table 4 summarizes the lyotropic phase behavior of the urea-based surfactants including the C6, C7,

**Figure 11.** 1-Decyl urea crystals in contact with water at 89 °C (optical microscopy with crossed polarizers; 100× magnification). Water penetrates from right to left. An isotropic liquid phase is well developed between the crystalline solid and water.**TABLE 4: Lyotropic Phase Behavior of the Alkyl Ureas^a**

surfactant	crystal–isotropic liquid transition (°C)
1-hexyl urea	74
1-heptyl urea	83
1-octyl urea	73
1-decyl urea	87
5-decyl urea	>100
1-dodecyl urea	89
2-dodecyl urea	95
4-dodecyl urea	>100
6- dodecyl urea	97

^a The transition refers to the temperature at which water penetrates the neat surfactant and an isotropic liquid is formed between the water and the solid crystalline surfactant.

and C8 1-alkyl ureas reported elsewhere.³¹ The temperatures for the first appearance of the isotropic surfactant–water phases, i.e., the crystal–isotropic liquid transition, are listed. The C6 and C8 1-alkyl ureas both exhibit similar transition temperatures and with the exception of the 1-heptyl urea, the transition temperatures increase with alkyl chain length. As 1-heptyl urea is the only urea-based surfactant with an odd number of carbons, this may be related to the “odd–even” effect commonly observed with the melting points for alternating odd- and even-numbered carbon compounds. The urea-based surfactants where the urea moiety is not located at the terminus of the hydrocarbon chain also have a higher crystal–isotropic liquid transition temperature than their 1-alkyl relatives. Nevertheless, examination of the dodecyl urea series of positional isomers does not reveal a consistent progression with urea moiety migration.

Conclusions

The impact of urea-based surfactant molecular geometry, specifically headgroup positional isomerism, on the solubility, melting point, and lyotropic phase behavior has been examined. It was initially speculated that structural isomerism in the alkyl chain may enhance the surfactant solubility in water. In fact, the opposite behavior was found. As was the case with the C6, C7, and C8 1-alkyl ureas,³¹ intermolecular hydrogen bonding between urea headgroups dominates the solid-to-isotropic liquid thermotropic transition of the longer-chain C10 and C12 ureas. Hydrogen bonding in the crystalline state is also responsible for the low solubility and a high crystal solubility boundary for these ureas in water. Interestingly, the urea surfactants where the urea moiety is not situated at the terminus of the hydrocarbon chain possess higher melting points.

Surfactant–water mixtures of the investigated urea-based surfactants, exhibit three phases, viz., a crystalline solid, a very dilute aqueous solution of the alkyl urea, and an isotropic liquid. The dilute solution and isotropic liquid coexist in the low-surfactant, high-temperature region of the phase diagram.

Acknowledgment. We thank George Georgaklis and Asoka Weerawardeena for obtaining some of the DSC data. We also thank Professor David Winkler for performing molecular modeling of the positional isomers. C.J.D. is the recipient of an Australian Research Council Federation Fellowship.

Supporting Information Available: Synthetic details. This material is available free of charge via the Internet at <http://pubs.acs.org>.

References and Notes

- (1) Kauffman, G. B.; Chooljian, S. H. *J. Chem. Educ.* **1997**, *74*, 1493.
- (2) Aylward, F.; Wood, P. D. S. *Nature* **1956**, *177*, 146.
- (3) Aylward, F.; Wood, P. D. S. *J. Appl. Chem.* **1957**, *7*, 583.
- (4) Aylward, F.; Wood, P. D. S. *J. Appl. Chem.* **1958**, *8*, 561.
- (5) Smith, A. E. *Acta Crystallogr.* **1952**, *5*, 224.
- (6) Zhao, X.; Chang, Y.-L.; Fowler, F. W.; Lauher, J. W. *J. Am. Chem. Soc.* **1990**, *112*, 6627.
- (7) Desiraju, G. R. *Angew. Chem., Int. Ed. Engl.* **1995**, *34*, 2311.
- (8) Chang, Y.-L.; West, M.-A.; Fowler, F. W.; Laughner, J. W. *J. Am. Chem. Soc.* **1993**, *115*, 5991.
- (9) Ahmad, B.; Ankita; Khan R. H. *Arch. Biochem. Biophys.* **2005**, *437*, 159.
- (10) Wang L. M.; Colon, W. *Protein Sci.* **2005**, *14*, 1811.
- (11) Chakraborty, A.; Sarkar, M.; Basak, S. *J. Colloid Interface Sci.* **2005**, *287*, 312.
- (12) Caballero-Herrera, A.; Nordstrand, K.; Berndt, K. D.; Nilsson, L. *Biophys. J.* **2005**, *89*, 842.
- (13) Mallam, A. L.; Jackson, S. E. *J. Mol. Biol.* **2005**, *346*, 1409.
- (14) Robinson, D. R.; Jencks, W. P. *J. Am. Chem. Soc.* **1965**, *87*, 2462.
- (15) Wetlaufer, D. B.; Malik, S. K.; Stoller, R. L. *J. Am. Chem. Soc.* **1964**, *86*, 508.
- (16) Liepinsch, E.; Otting, G. *J. Am. Chem. Soc.* **1994**, *116*, 9670.
- (17) Shen, X. H.; Belletete, M.; Durocher, G. *J. Phys. Chem.* **1997**, *101*, 8212.
- (18) Wallqvist, A.; Covell, D. G.; Thirumalai, D. *J. Am. Chem. Soc.* **1998**, *120*, 427.
- (19) Quintana, R. P.; Fisher, R. G.; Lasslo, A. *J. Colloid Interface Sci.* **1973**, *44*, 443.
- (20) Alexander, A. E. *Proc. R. Soc. Ser. A* **1941**, 470.
- (21) Adam, N. K. *Proc. R. Soc. Ser. A* **1922**, 452.
- (22) Hunter D. S.; Barnes G. T.; Godfrey J. S.; Grieser F. *J. Colloid Interface Sci.* **1990**, *138*, 307.
- (23) Shimizu, M.; Yoshida, M.; Limura, K.; Suzuki, N.; Kato, T. *Colloids Surf., A* **1995**, *102*, 69.
- (24) Urai, Y.; Ohe, C.; Itoh, K.; Yoshida, M.; Iimura, K.; Kato, T. *Langmuir* **2000**, *16*, 3920.
- (25) Stosch, R.; Cammenga, H. K. *J. Colloid Interface Sci.* **2000**, *230*, 291.
- (26) Seki, T.; Fukuchi, T.; Ichimura, K. *Langmuir* **2002**, *18*, 5462.
- (27) Seki, T.; Fukuchi, T.; Ichimura, K. *Langmuir* **2000**, *16*, 3564.
- (28) Kobayashi, Y.; Seki, T. *Langmuir* **2003**, *19*, 9297.
- (29) Huo, Q.; Russev, S.; Hasegawa, T.; Nishijo, J.; Umemura, J.; Puccetti, G.; Russell, K. C.; Leblanc, R. M. *J. Am. Chem. Soc.* **2000**, *122*, 7890.
- (30) Wang, Y.; Wang, C.; Wang, X.; Guo, Y.; Xie, B.; Cui, Z.; Liu, L.; Xu, L.; Zhang, D.; Yang, B. *Chem. Mater.* **2005**, *17*, 1265.
- (31) Wells, D.; Drummond, C. J. *Langmuir* **1999**, *15*, 4713.
- (32) Fong, C.; Wells, D.; Krodiewska, I.; Hartley, P. G.; Drummond, C. J. *Chem. Mater.* **2006**, *18*, 594.
- (33) Wells, D.; Fong, C.; Krodiewska, I.; Drummond, C. J. Nonionic Urea Surfactants: Formation of Inverse Hexagonal Lyotropic Liquid Crystalline Phases by Introducing Hydrocarbon Chain Unsaturation. *J. Phys. Chem. B*, submitted for publication.
- (34) Davis, T. L.; Blanchard, K. C. *J. Am. Chem. Soc.* **1929**, *51*, 179.
- (35) Buck, J. S.; Ferry, C. W. *J. Am. Chem. Soc.* **1936**, *58*, 854.
- (36) Silverstein, R. M.; Bassler, G. C.; Morrill, T. C. *Spectrometric identification of organic compounds*, 4th ed.; John Wiley and Sons: New York, 1981.
- (37) Mido, Y.; Murata, H. *Nippon Kagaku Zasshi (J. Chem. Soc. Jpn., Pure Chem. Sect.)* **1969**, *90*, 254.
- (38) Mido, Y.; Murata, H. *Bull. Chem. Soc. Jpn.* **1969**, *42*, 3372.
- (39) Mido, Y. *Spectrochim Acta* **1973**, *29A*, 1.
- (40) Mido, Y. *Spectrochim Acta* **1972**, *28A*, 1503.
- (41) Hashimoto, M.; Tajima, F.; Eda, K.; Yamamura, K.; Okazaki, T. *J. Mol. Struct.* **2005**, *734*, 23.
- (42) Feuer, H.; Rubinstein, H.; Nielson, A. T. *J. Org. Chem.* **1958**, *23*, 1107.
- (43) Buck, J. S.; Hjort, A. M.; Id, e W. S.; deBeer E. J. *J. Am. Chem. Soc.* **1938**, *60*, 461.
- (44) Weast, R. C. *CRC Handbook of Chemistry and Physics*, 60th ed.; CRC Press: Boca Raton, FL, 1981.
- (45) Tanford, C. *The Hydrophobic Effect: Formation of Micelles and Biological Membranes*; Wiley-Interscience, New York, 1973.
- (46) Laughlin, R. G. *The Aqueous Phase Behaviour of Surfactants*; Academic Press: San Diego, 1996.
- (47) Boyd, B. J.; Drummond, C. J.; Krodiewska, I.; Weerawardena, A.; Furlong, D. N.; Grieser, F. *Langmuir* **2001**, *17*, 6100.
- (48) Hommelen, J. R. *J. Colloid Sci.* **1959**, *14*, 385.
- (49) Rosen, M. J. *Surfactants and Interfacial Phenomena*; Wiley-Interscience: New York, 1978.